Food Hydrocolloids 166 (2025) 111320

Contents lists available at ScienceDirect

Food Hydrocolloids

journal homepage: www.elsevier.com/locate/foodhyd

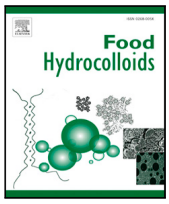

The role of pea protein content and carbohydrate molecular weight in the structure and stability of spray-dried emulsions

T. Kurtz [a,*], K. Haas [b], J. Busom Descarrega [b], V. Meunier [b], O. Schafer [b], S. Heinrich [a]

[a] Institute of Solids Process Engineering and Particle Technology, Hamburg University of Technology, Denickestraße 15, Hamburg, 21073, Germany
[b] Nestlé Research Center, Vers-Chez-Les-Blancs, Lausanne, 1000, Switzerland

ARTICLE INFO

Keywords:
Microencapsulation
Free fat
Oxidation
Beta carotene
Protein aggregation
Oxygen diffusion

ABSTRACT

With increasing interest to replace dairy proteins in food products, questions of performance and stability of these alternatives rise. Plant-based proteins and carbohydrates that are used for dried emulsion systems, like plant-based milk or creamer powder, are expected to influence micro structure of final powders with further impact on storage stability. The aim of this work was to investigate the plant-based matrix, with focus on pea protein content and carbohydrate molecular weight, on spray-dried powder structure, fat distribution and oxidation stability of the bioactive component beta carotene. Spray-dried powders were produced from plant-based emulsions with varying protein content (2.4, 20% wt) and maltodextrin dextrose equivalent (DE 6, 21, 40). Both factors significantly impacted particle structure and free fat content of spray-dried powders. While the effect on structure and morphology did not follow clear trends, free fat differed greatly between powders (4.5–88.8%) and showed to increase with protein content and decreased maltodextrin DE. Beta carotene stability during storage followed similar trends, with highest retention after storage measured for coarse, low protein and maltodextrin DE 40 powder (37.9%), while poorest performance was found for powders with maltodextrin DE 6 (9.5–12.3%), independent of the protein content. The study showcases the high impact of carbohydrate molecular weight and plant proteins on structure and thus stability indicators of plant-based powders. For a sustainable substitution of dairy protein in food powders, these differences need to be considered during processing and production.

1. Introduction

In recent years, there has been increased interest by consumers to replace bovine milk and its products with plant-based alternatives (Aydar et al., 2020; Sethi et al., 2016). In milk alternatives, the principal components, which include dairy protein, milk fat and lactose, are replaced by plant-based counterparts such as sugars or maltodextrins, vegetable oils and plant proteins. Plant proteins used in such applications can be derived from a wide selection of plant sources, such as cereals, legumes and pulses. Among these, pea protein is a promising candidate due to its high nutritional value, low cost and good availability (Akharume et al., 2021).

While there are numerous advantages associated with the use of plant proteins, such as health benefits, improved sustainability and increased animal welfare (Boukid et al., 2022), techno-functional properties of these “new” proteins can differ vastly. In contrast to dairy proteins, emulsions containing pea protein isolate have relatively coarse fat droplet size distributions and are further prone to flocculation and aggregation, which are considered detrimental to emulsion quality (Bernaschina et al., 2024; Burger & Zhang, 2019; Hinderink, Schröder, et al., 2021). While there are several processing routes that can improve the functional properties of pea proteins (e.g. enzymatic hydrolysis), untreated proteins are considered beneficial from an economic and sensory aspect (Vogelsang-O’Dwyer et al., 2022; An et al., 2024). Lately, liquid emulsions stabilized by plant proteins, which can be used as milk substitutes, were widely studied (Bernaschina et al., 2024; Kramm et al., 2024), while their application and impact in dried product formulations and especially the shelf life of dry products is less understood.

The most common technique to produce (plant-based) milk powders is spray drying, providing the obtained powders with a favorable particle size distribution, bulk density, and dispersibility compared to other drying techniques (Binesh et al., 2023). In spray-dried particles, oil droplets are embedded (encapsulated) within a wall material of proteins and carbohydrates, while some lipids remain on the particle surface or in cracks. Key factors impacting powder stability, which are linked to the generated powder structure, were identified in previous

* Corresponding author.
E-mail address: teresa.kurtz@tuhh.de (T. Kurtz).

https://doi.org/10.1016/j.foodhyd.2025.111320
Received 16 October 2024; Received in revised form 11 February 2025; Accepted 3 March 2025
Available online 15 March 2025

studies: Powder particle size or morphology (Linke et al., 2020b; Jafari et al., 2007; Abd Ghani, Adachi, Sato, et al., 2017; Fang et al., 2005; Haas et al., 2019; Haas et al., 2020), encapsulation efficiency or free fat content (Shiga et al., 2017; Drusch & Berg, 2008), diffusion of oxygen through the particle wall (e.g. Hogan et al., 2001; Danviriyakul et al., 2002; Drusch et al., 2009; Abd Ghani, Adachi, Shiga, et al., 2017; Laina et al., 2024) as well as the interfacial layer are considered crucial for powder stability. Furthermore, oil droplet size of the feed emulsion has been found to impact both encapsulation efficiency and oxidation stability (Linke et al., 2021; Linke et al., 2020c; de Barros Fernandes et al., 2014; Abd Ghani, Adachi, Shiga, et al., 2017; Kikushi et al., 2013; Schröder et al., 2012). Noteworthy, most of the named factors are highly impacted by the level and type of "wall material", which are in case of plant-based milk alternatives, the plant proteins and carbohydrates added. While most studies merely focus on one of these factors, there is currently a lack of knowledge regarding the combination of different impact factors and their interrelation, particularly when it comes to the incorporation of high molecular weight (Mw) plant proteins into the matrix.

The aim of this study was therefore to investigate the impact of different levels of pea protein isolate in combination with different molecular weight carbohydrates on powder characteristics and stability of milk alternative systems. For this purpose, model emulsions with varying protein content of pea protein isolate and Mw distribution of the carbohydrates were spray-dried and characterized in terms of particle morphology, free fat content and oxidation stability. Mw distribution was altered by using maltodextrin with different dextrose equivalents (DE), where higher DE corresponds to a higher degree of hydrolization and thus reduced Mw (Avaltroni et al., 2004). To further take into account the effect of structure, fine and coarse powder fractions were collected. Special care was further taken to decouple the effect of the matrix (e.g. viscosity, protein content) on the homogenization outcome and the particle structure formation during drying, by adding the main part of the matrix after the emulsification of the oil phase.

2. Materials and methods

2.1. Materials

For the purpose of this study, a plant-based milk alternative model system was developed, using pea protein isolate (Pisane C9), maltodextrin and sunflower oil. To monitor storage stability, beta-carotene (BC) powder was dissolved within the lipid phase. Pea protein isolate had a proximate composition of 80% protein, 9% residual lipids and 1.4% dietary fiber (Schumacher et al., 2025) and was provided by Cosucra (Warcoing, Belgium). Sunflower oil was kindly gifted from C. Thywissen GmbH (Neuss, Germany). Maltodextrins with DE of 6 (Glucidex DE6), 21 (Glucidex IP21) and 40 (Glucidex DE40) were purchased from Roquette (Lestrem, France). BC powder (≥ 93%) was obtained from Sigma Aldrich (Saint Louis, MO, USA). All chemicals used for carotenoid and surface fat extraction were of analytical grade and purchased at Carl Roth GmbH & Co. KG (Karlsruhe, Germany). Within this study, two different protein contents (low (2.4%) and high (20%)) were investigated. Additionally, maltodextrins with differing dextrose equivalents (DE) (6, 21, 40) were used to change the molecular weight (Mw) distribution of the matrix. Even though some of the used materials are considered as glucose syrup (DE 21, DE 40) from a regulatory point of view, for simplification they will be referred to as maltodextrin. In order to mimic a whole fat milk powder, fat content was set to 28% in all powders. In total, 6 recipes were formulated and produced in duplicates (Table 1).

Table 1
Formulations of different emulsions (wt/wt of dry matter).

Lipid (%)	BC (% oil)	Protein (%)	Maltodextrin (%)	DE (–)
28	0.05	2.4	69.6	6
				21
				40
		20	52	6
				21
				40

2.2. Emulsion preparation

In order to decouple impact of emulsion structure and other matrix effects on the morphology development and stability of the spray-dried emulsions, it was aimed to keep oil droplet size similar across all produced emulsions, through an emulsion preparation procedure that minimizes the impact of protein content and maltodextrin DE on the oil droplet size (Fig. 1). Firstly, base emulsions composed of 40% of total water, 2.4% protein and sunflower were produced for all recipes. For this, protein was dispersed in water and stirred with an overhead stirrer (Ministar®, IKA, Staufen, Germany) at 300 rpm for 30 min. The suspensions were further refrigerated and hydrated overnight. Oil-in-water emulsions were prepared by addition of sunflower oil (28% wt/wt of total solids) containing 0.05% BC (wt/wt of oil phase) to the hydrated protein suspension and shearing for 5 min. The emulsion was consecutively homogenized in two passages at 250/50 bar in a high-pressure homogenizer (HPH) (Panda Plus, Gea, Düsseldorf, Germany). The conditions for emulsion preparation (solids content, HPH pressure) were determined through preliminary experiments (data not shown).

Secondly, a protein dispersion and a maltodextrin dispersion were produced for high and low protein samples respectively. For high protein samples, remaining protein (17.6%) and remaining 60% of total water were combined, stirred for 30 min at 300 rpm with an overhead stirrer and further hydrated over night in the fridge. Maltodextrin was added and the mixture sheared for 5 min at 9000 rpm with a rotor-stator disperser until total dissolution of maltodextrin, before being homogenized in two passages at 350/100 bar in a high-pressure homogenizer.

For low protein samples, maltodextrin was combined with remaining 60% of total water and sheared until total dissolution. Lastly, the base emulsion was combined with the maltodextrin or protein suspension by gentle stirring. All final emulsions had a total solids (TS) content of 35% and were produced in duplicates.

2.3. Drying

Spray-drying was performed in duplicates for each recipe in a pilot-scale spray dryer (Niro minor, Søborg, Denmark) equipped with a two-fluid nozzle operated at 2 bar atomizing pressure, following the procedure of Haas et al. (2019). A total of 5 kg emulsion was dried per trial at a feed flow rate of 58 – 77 mL/min. Inlet temperature was maintained at 190 °C and the outlet temperature varied between 60 – 70 °C. Two different size fractions were collected. The larger particles were collected from the bottom outlet of the drying chamber, while the finer particles were separated from the process air and collected through a cyclone, leading to a total of 12 samples in duplicates.

2.4. Emulsion and powder characterization

Particle size distribution (PSD) of the emulsions before and after spray-drying was characterized using laser diffraction (Mastersizer3000, Malvern Panalytical, Malvern, United Kingdom). The prepared emulsions were dispersed in a dispersion unit filled with water at constant agitation and 5 consecutive measurements were performed for each sample. The PSD was calculated with an algorithm based on

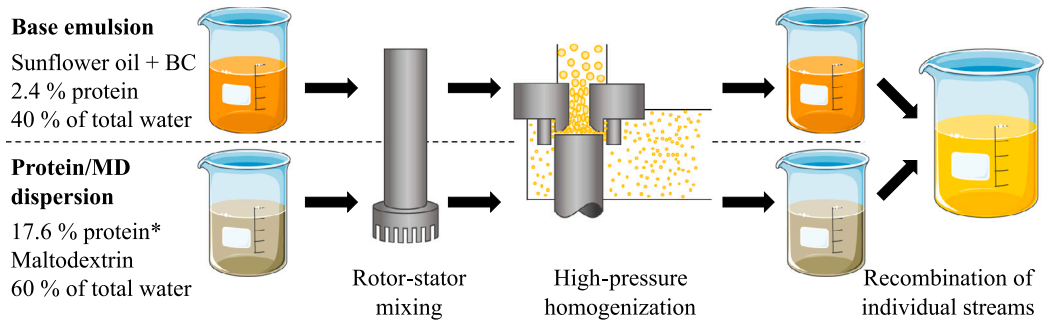

Fig. 1. Schematic representation of emulsion production. * Addition of protein only refers to high protein samples.

the Mie theory using a refractive index of sunflower oil of 1.6 and 1.33 for water. Surface mean diameter ($d_{3,2}$) and the volume mean diameter ($d_{4,3}$) were used to describe the distribution.

Emulsion viscosity was determined with a Kinexus Pro rheometer (Malvern Panalytical, United Kingdom), equipped with a concentric cylinder geometry. Up and downward viscosity curves were measured and values at a shear rate of 630 s^{-1} of downward curve were used for comparison.

Powder particle size was determined by dynamic image analysis (Camsizer XT, Microtrac Retsch GmbH, Haan, Germany). Powder samples were dispersed using pressurized air and analyzed by two high speed cameras capturing large and small particles. The diameter of a circle with an identical area (x_{area}) was used for evaluation and calucualtion of the median diameter ($d_{50,3}$) as well as the surface mean diameter ($d_{3,2}$). To ensure measurement of individual particles, 0.5% wt/wt of silicon dioxide was added as a flowing agent.

Residual moisture content (x_{res}) was measured in triplicates. 2 g of powder were weighed into aluminum dishes and dried for 24 h at 103 °C, cooled down in a desiccator and weighed. Moisture content was determined from weight difference before and after drying. Sorption isotherms were determined using the BET model (Brunauer et al., 2000) with a method established by Dupas-Langlet et al. (2016) and were used to calculate water activity of produced powder samples. Glass transition temperature (T_g) was calculated using the Gordon-Taylor model (Gordon & Taylor, 1952).

The apparent density (ρ_a) as well as the material density ($\rho_{material}$) were measured using a helium pycnometer (AccuPyc 1330, Micromeritics, Norcross, GA, USA) equipped with a 3.5 cm^3 sample cup at 1.38 bar using Boyle-Mariotte law. While for ρ_a powder was measured as is, powder was ground in a mortar before measurement to expose all inner pores and to obtain the true material density. Measured values were used to calculate the volumetric fraction of closed pores (closed porosity), which are not connected to the particle surface, according to Eq. (1):

$$Closed\ porosity\,(\%) = \left(1 - \frac{\rho_a}{\rho_{material}}\right) \cdot 100\% \quad (1)$$

2.5. Free fat content

Non-encapsulated fat generally shows different degradation behavior compared to encapsulated fat. The determination of free fat content is thus considered of importance for comparative shelf-life studies. Free fat was determined gravimetrically in triplicates using heptane extraction, following a protocol by Sarkar et al. (2016) with some modifications: Approximately 2 g of powder were weighed into screw cap glass bottles and 40 mL of heptane were added. Mixtures were shaken for 10 min using a lab shaker KL-2 (Edmund Bühler, Germany) to ensure good exposure of powder particles to solvent. After shaking, powder was decanted and heptane phase filled into 50 mL centrifuge tubes with consecutive centrifugation for 5 min at 2000 rpm. The clear supernatant was filtered from remaining powder particles using a 45 nm syringe filter. 25 mL of heptane solution were evaporated in weighed aluminum dishes at 110 °C. After complete visual evaporation, remaining solvent traces were removed by drying in a laboratory oven at 100 °C for 30 min and left to cool in a silica desiccator for a minimum of 1 h. Free fat content was calculated based on total theoretical lipid content.

2.6. Oxidation stability

In order to monitor stability of encapsulated ingredients over the course of storage, BC was used as model vitamin and it's oxidation monitored over a storage period of 84 days at standardized conditions of 35 °C and 20% relative humidity. BC degradation was analyzed spectrophotometrically using an extraction procedure described by Sarkar et al. (2016) with some modifications: For total BC extraction, powders were dissolved in reaction vials with demineralized water containing 0.1% sodium ascorbate as antioxidant, using a rotor-stator disperser (IKA ULTRA-TURRAX®, Staufen, Germany) at 9000 rpm for 2 min. The solution was transferred to a 50 mL volumetric flask and filled up to the mark with demineralized water. The final dry matter content was between 6 – 8%. From each solution, BC was extracted in triplicates. For this, 2 mL of the prepared solution was mixed with 10 mL of an extraction mixture containing acetone, ethanol, and heptane in a ratio of 7:3:10 with 0.025% butylhydroxytoluol (BHT) as additional antioxidant. Solution and solvent mixture aliquots were combined in a screw cap glass vial and vigorously shaken by hand for 45 s. Vials were afterwards placed in an ultrasonic bath for 15 s to improve phase separation. Upper phase was consecutively washed with 10% wt/wt NaCl-solution and the washed heptane phase was transferred to light-excluding reaction vials. Beta-carotene absorption of the extracts was measured at the wavelength of maximal absorbance (λ_{max}) at 450 nm in a spectrophotometer (GENESYS 10, Thermo Electron, WI, USA).

Encapsulated and non-encapsulated (free) BC are known to oxidize at significantly different rates (Haas et al., 2019). In order to be able to determine the oxidation of encapsulated beta carotene, which is influenced by diffusion through the particle wall, free BC was measured. 0.5 g of powder was weighed in duplicates into light excluding centrifuge vials and 20 mL of heptane were added. The mixture was shaken on a laboratory shaker for 10 min at 150 rpm. To remove all remaining particles, the upper phase was first decanted into another centrifugal vial and centrifuged for 5 min at 2000 rpm and consecutively filtered through a 45 nm syringe filter. The obtained solution was measured at 450 nm in a spectrophotometer. Encapsulated BC was calculated from the difference of total and free BC.

2.7. Microstructural analysis

To observe droplet size and protein aggregation, emulsions were examined using a light microscope (BX51, Olympus, Japan) in transmission mode at 100 fold magnification. To image the emulsions, one drop of diluted sample was directly place between a microscopy slide and a cover slide.

Table 2
Particle size and viscosity of protein dispersion and base emulsions after homogenization as well as recombined emulsion for different formulations.

Protein content	Maltodextrin DE	Protein dispersion		Base emulsion		Recombined emulsion		Viscosity at 630 s-1
(%)	(–)	$d_{3,2}$ (μm)	$d_{4,3}$ (μm)	$d_{3,2}$ (μm)	$d_{4,3}$ (μm)	$d_{3,2}$ (μm)	$d_{4,3}$ (μm)	(mPa s)
2.4	6	–	–	7.4 ± 0.1^{a}	10.4 ± 0.1^{a,b}	5.5 ± 0.8	13.7 ± 3.8	85.7
2.4	21	–	–	4.6 ± 1.1^{c}	6.6 ± 1.3^{b}	6.2 ± 1.3	9.5 ± 2.6	21.1
2.4	40	–	–	5.2 ± 0.5^{b,c}	15.4 ± 5.1^{a}	5.6 ± 0.2	8.8 ± 0.1	12.8
20	6	15.7 ± 5.3	51.1 ± 12.6	4.8 ± 0.9^{b,c}	7.1 ± 1.2^{b}	6.2 ± 0.7	28.2 ± 4.7	217.3
20	21	3.6 ± 3.7	19.4 ± 10.2	5.1 ± 2.0^{b,c}	7.3 ± 2.1^{b}	7.2 ± 0.2	17.8 ± 1.2	89.0
20	40	2.2 ± 3.2	19.6 ± 10.6	6.6 ± 0.4^{a,b}	15.4 ± 2.7^{a}	4.9 ± 0.2	10.6 ± 0.2	56.4

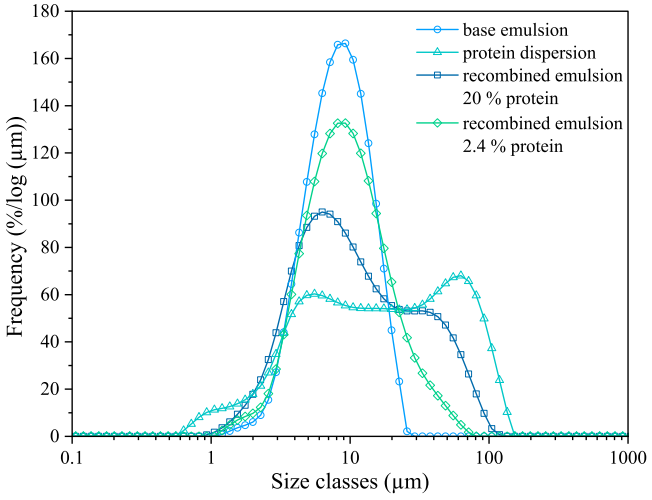

Fig. 2. Size distribution of base emulsion, protein dispersion and recombined emulsion for a recipe containing 20% protein and maltodextrin DE 21 and a recombined emulsion containing 2.4% protein.

Fluorescence microscopy was used to investigate the spatial distribution of proteins and lipids by being stained with Fast Green (FG) and Nile Red (NR) respectively. Fast green FCF (Sigma–Aldrich, Zwijndrecht, The Netherlands) was diluted at 1 mg/mL in deionized water and Nile red (Sigma–Aldrich, Zwijndrecht, The Netherlands) was diluted at 0.25 mg/mL in ethanol (Fisher Scientific, Landsmeer, The Netherlands). 1 mL of sample stained by the addition of 10 μl of FG solution followed by 10 μl of NR solution. The sample was then covered by a microscopy glass slide before observation with a LSM710 upright confocal microscope equipped with an Airyscan detector (Zeiss, Oberkochen, Germany) using Plan-APOCHROMAT objectives (10x/0.45, 20x/0.8, 63x/1.4) and 488 nm and 633 nm excitation laser lines for NR and FG, respectively. Images were analyzed with the ZEN imaging software (Zeiss, Oberkochen, Germany).

For visualization of surface lipids, powder samples were stained using osmium tetroxide (OsO_4), a method first described by Palade (1951). OsO_4 increases contrast between lipids and non-lipids and lets lipid rich areas appear brighter on SEM images. Powders were fixated on an aluminum sample holder using conductive carbon stickers and lightly tapped with a razor blade to expose the inner particle structure. Specimen holders were placed in a desiccator and exposed to OsO_4 vapor overnight. Powders were consecutively analyzed under a Scanning Electron Microscope (SEM) Quattro S (Thermo Fisher, United States) at an accelerating voltage of 10 kV and employing a back-scattered electron detector. Low-vacuum mode was employed to reduce charging artifacts.

2.8. Statistical evaluation

All powders were produced in duplicates. Results were reported in mean ± standard deviation unless stated otherwise. Statistical analysis of selected data sets was carried out using one-way Analysis of Variance (ANOVA) with $\alpha = 0.05$.

3. Results and discussion

3.1. Emulsion characteristics

The structure and morphology of spray-dried particles is largely influenced by the properties of the emulsion, thus a good understanding of emulsion characteristics is crucial. Table 2 summarizes characteristic particle sizes ($d_{3,2}$ and $d_{4,3}$) of intermediate emulsion products and final recombined emulsions as well as emulsion viscosity. Full viscosity curves can be found in Supplementary information 3. Representative particle size distribution curves of an exemplary recipe containing maltodextrin DE 21 are shown in Fig. 2 and corresponding light microscopic images of base emulsion, protein dispersion and recombined emulsion for a 2.4% and 20% formulation in Fig. 3.

$D_{3,2}$ values of protein dispersions, which do not contain oil, increased with decreasing DE of used maltodextrin from 2.2 ± 3.2 μm to 15.7 ± 5.3 μm and $d_{4,3}$ from 19.4 ± 10.2 μm to 51.1 ± 12.6 μm. Protein dispersions before HPH were very large and exhibited a $d_{3,2}$ and $d_{4,3}$ of 89 μm and of 169 μm respectively (Supplementary information 2), which indicates a generally good break-up of protein aggregates during homogenization, while some large aggregates still remain. This is also visualized in light microscopic images (Fig. 3 b), where mostly small and broken-up and only few large aggregates are visible. Particle size distributions of protein dispersions after HPH are polymodal with distinct peaks around 70 μm, 5 μm and a smaller shoulder around 1 μm (Fig. 2). The small shoulder around 1 μm may be related to small oil droplets that remained in the protein isolate after extraction and that are inherently stabilized by in-situ polar compounds. These lipids range around 9% according to protein supplier documentation. Another possibility could be very small aggregates that were generated during homogenization. The two larger peaks likely characterize the different break-up states of protein aggregates, which is also reflected in $d_{3,2}$ and $d_{4,3}$ values (Table 2). These globular aggregates are formed during the extraction process to produce plant proteins through the aggregation of non-polar amino-acid groups, which lead to the formation of insoluble complexes (Yang et al., 2024; Burger et al., 2022). High pressure homogenization can break up these large structure into smaller, more soluble aggregates (Yang et al., 2024; Keuleyan et al., 2023; D'Alessio et al., 2023). The effectiveness of this break-up during high pressure homogenization seems however to be dependent on the DE value of maltodextrin, since $d_{3,2}$ and $d_{4,3}$ increase with increasing maltodextrin Mw (Table 2). Maltodextrin is water soluble and thus not expected to generate any signal response during laser diffraction. This effect therefore more likely results from the increase in viscosity as imposed by higher Mw (Avaltroni et al., 2004), which hinders an effective aggregate breakup due to changes in the flow regime during homogenization (Coccaro et al., 2018). Gavi et al. (2018) found that higher viscosity strongly limited the break up of nanoparticle clusters using a microfluidizer.

For base emulsion, average $d_{3,2}$ was relatively stable around 5.4 ± 1.4 μm, while higher fluctuations were observed for $d_{4,3}$ of

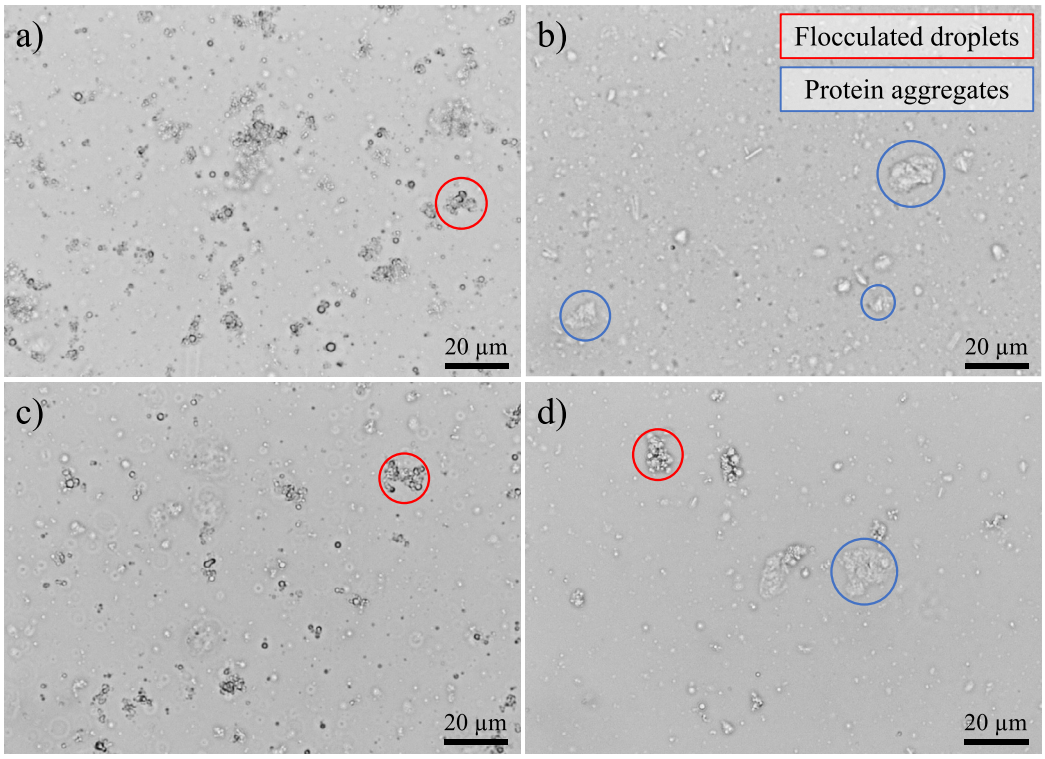

Fig. 3. Light microscopic images taken at 100-fold magnification of base emulsion after homogenization (a), protein dispersion after homogenization (b) and recombined emulsions with 2.4% protein (c) and 20% protein (d) of an exemplary recipe containing maltodextrin DE 21.

10.0 ± 4.7 µm, which may indicate an overall constant size of primary droplets and higher variations through droplet clusters and aggregates. Particle size distribution (Fig. 2) was mono-modal with a peak around 8 µm, which is in accordance with droplet size distributions obtained with pea protein isolate by other authors (Cao et al., 2025). The light microscopy images likewise show that base emulsions exhibit small, single oil droplets in the range of 1 to 2 µm as well as several larger aggregated droplets. Since individual droplets are still visible within those aggregates, it can be assumed that they are caused by flocculation (McClements et al., 2019; Bernaschina et al., 2024). Droplets are larger than the emulsions produced with more classical emulsifiers like whey protein isolate since globular proteins are considered less flexible and require more time to adsorb at the interface (Hinderink, Berton-Carabin, et al., 2021). The oil droplet size observed in light microscopic images is considerably smaller than values estimated from laser diffraction measurements, which can be attributed to the impact of flocculated droplet clusters, which affect mean values. Additionally, it is still possible that some large protein aggregates remain even at low protein concentrations which can dramatically affect $d_{4,3}$ values due to their large volume.

The final recombined emulsion is consequently bi-modal, whereas the first peak around 7 µm can be attributed to oil droplets and the second peak around 12 µm to the presence of non-dissolved aggregates and flocculated droplets, even though actual oil droplet size is likely to be much smaller according to light microscopy images, as previously discussed. The different break-up efficiencies of the protein dispersion are also represented in the increasing $d_{4,3}$ values with decreasing maltodextrin DE (Table 2). It is also possible that bridging flocculation further increased through the increased amount of protein in the emulsion. Recombined emulsions containing 2.4% protein on the other hand remained monomodally distributed since no further protein was added but just solubilized maltodextrin, which did not affect droplet size distribution. It should be mentioned, that while laser diffraction is a useful tool to measure particle sizes of emulsions, for polydisperse systems like the present one, containing single droplets as well as droplet clusters and aggregates, data interpretation remains challenging.

Based on microscopy images, it appears that oil droplet size is in the same order of magnitude for the different compositions. However, over-all emulsion structure varied greatly between high and low protein formulations. Low protein emulsions were predominantly governed by single and flocculated droplets, whereas high protein formulations were further impacted by different amounts of non or partly broken up protein aggregates.

3.2. Influence of protein content and wall material on powder properties

In order to obtain two different particle size fractions from each spray-drying trial, powder was collected both from the bottom outlet of the drying chamber (coarse fraction) and after cyclone separation (fine fraction). Table 3 summarizes $d_{50,3}$ and $d_{3,2}$ values for obtained coarse and fine powder fractions. $D_{50,3}$ values for coarse powder fractions increased with decrease of maltodextrin DE from 51.8 to 93.1 µm for low protein powders and from 55.2 to 69.3 µm for high protein powders. Fine powder fractions were in a very similar range from 18.4 to 22.7 µm, with no particular trend for protein content or maltodextrin DE, resulting in two distinctly sized powder fractions for each recipe.

As discussed in Section 2.2, emulsion viscosity increased with protein content and decreasing maltodextrin DE. Increased viscosity through higher Mw carbohydrates is generally associated with larger particles after spray drying (Serfert et al., 2009). Consecutively, it would be expected to obtain the largest particles for high protein and DE 6 samples, which is however not reflected in the present data. While DE 6 powders were generally larger than powders with lower DE values and high protein powders generally larger than low protein powders, largest particles were obtained with low protein content and DE 6. Reason for this could be involuntary agglomeration of particles during the spray-drying process, during which single particles form larger units through formation of solid bridges (e.g. sintering). This hypothesis is supported through SEM images of coarse powders (Fig. 4), where

Table 3
Properties of produced powders. $d_{50,3}$ and $d_{3,2}$ are expressed as means with mean deviation, all other values as means with standard deviation. Different letters represent significant differences at 0.05 level.

Protein content (%)	DE (–)	Size fraction (–)	$d_{50,3}$ (μm)	$d_{3,2}$ (μm)	x_{res} (%)	ρ_{app} (g cm^{-3})	ϵ_{closed} (%)
2.4	6	coarse	93.1 ± 18.8^{a}	64.9 ± 8.3^{a}	3.1 ± 0.5	0.946 ± 0.024	10.7 ± 3.7
2.4	6	fine	21.6 ± 0.0^{c}	17.1 ± 0.0^{c}	3.2 ± 0.7	1.128 ± 0.006	4.2 ± 0.7
2.4	21	coarse	52.2 ± 5.1^{b,c}	40.3 ± 3.2^{a,b,c}	2.3 ± 0.2	1.040 ± 0.008	10.2 ± 1.7
2.4	21	fine	18.4 ± 0.1^{c}	14.6 ± 0.1^{c}	2.3 ± 0.1	1.227 ± 0.004	2.8 ± 0.4
2.4	40	coarse	51.8 ± 1.2^{b,c}	40.1 ± 0.1^{a,b,c}	2.0 ± 0.2	1.146 ± 0.007	9.2 ± 1.2
2.4	40	fine	22.6 ± 3.1^{c}	22.5 ± 6.1^{b,c}	2.0 ± 0.1	1.271 ± 0.003	2.5 ± 1.3
20	6	coarse	69.3 ± 7.8^{a,b}	49.6 ± 9.1^{a,b}	1.9 ± 0.6	0.992 ± 0.007	7.1 ± 1.3
20	6	fine	21.7 ± 1.1^{c}	17.5 ± 0.7^{c}	3.3 ± 0.1	1.171 ± 0.009	4.0 ± 1.2
20	21	coarse	69.7 ± 2.6^{a,b}	54.1 ± 3.2^{a}	1.2 ± 0.1	0.958 ± 0.031	9.5 ± 5.5
20	21	fine	22.7 ± 4.2^{c}	20.3 ± 6.1^{c}	2.1 ± 0.1	1.122 ± 0.022	4.2 ± 2.4
20	40	coarse	55.2 ± 11.9^{a,b,c}	41.9 ± 7.7^{a,b,c}	1.0 ± 0.4	1.028 ± 0.014	9.4 ± 1.3
20	40	fine	19.6 ± 0.8^{c}	13.9 ± 0.7^{c}	1.8 ± 0.1	1.150 ± 0.020	5.3 ± 3.1

more numerous and larger agglomerates can be observed for low than for high protein powders. Proteins tend to accumulate at the particle surface during spray-drying and can prevent the formation of viscous bridges between particles and thus the formation of agglomerates (Kim et al., 2009; Drusch et al., 2012).

Residual powder moisture content can be considered low for all samples and decreased with decreasing MW distribution of the carrier, as already reported by other authors (Rodríguez-Hernández et al., 2005; Werner et al., 2007). Moisture content was generally lower for high protein than for low protein samples, which may be due to the reduced quantity of maltodextrin, which can potentially improve water diffusion during drying (Gianfrancesco et al., 2012). Water activity was below 0.12 for all samples and T_g ranged from 60 °C (2.4% protein, DE 40) to 150 °C (2.4% protein, DE 6) (Supplementary information 1).

Previous studies have shown that porosity usually increases with increased emulsion viscosity as well as lower maltodextrin DE, due to the formation of larger vacuoles and a faster film formation of materials with higher glass transition temperature (Abd Ghani, Adachi, Shiga, et al., 2017; Serfert et al., 2009). This trend was observed for the samples with low protein content but not for samples with 20% of protein. The smaller particles from the fine fraction show generally lower closed porosity compared to the coarse fraction, which is most likely due to a structure interlocking at lower residue moisture of the particles. The absence of a clear trend in closed porosity for the samples indicate either a possible increase in open porosity, meaning pores and cracks on the particle surface that form channels through the particle and also access vacuoles inside the particles, or an increased gas permeability of the matrix, enabling the penetration of gas during the measurement.

Material density describes the true density of a material without any enclosed pores. The differences in the material density (as shown in Fig. 5) of the samples can be explained by the matrix free volume, which is the volume of the total mass that is occupied by micro- and nanocavities rather than polymer chains and is related to the stability of a matrix towards gas diffusion (Drusch et al., 2009; Dlubek et al., 2002). Free volume of a glassy carbohydrate, such as maltodextrin, is decreasing with decreasing chain length of the polymer, as this induces a denser molecular packing and consequently reduces the diffusion of small molecules such as oxygen through the particle wall (Drusch et al., 2009). Large polymers within the matrix, such as proteins, can increase free volume elements and thus lower material density, which correlates to generally lower density values of high protein samples (Drusch et al., 2012).

3.3. Free fat content

The quantity of free, non-encapsulated lipids presents an important powder property as it can impact powder flowability but also the stability of lipids and other oxidation sensitive compounds in a powder. Buma (1971) and Drusch and Berg (2008) have shown that free fat is located at the particle surface and in the interior, where it might be accessible for extraction through sub-micro pores and cracks. Free fat content of spray-dried powders is presented in Fig. 6 and ranged from 4.5 ± 1.3% (2.4% protein, DE 40, coarse) to 88.8 ± 2.4% (20% protein, DE 6, fine). Protein content as well as particle size and DE-value significantly impacted free fat content of produced powders (p-value <0.05). For all powders, fine powder fractions exhibited higher free fat contents than corresponding coarse powders, which is likely related to the higher surface to volume ratio of smaller particles and consequently a higher probability of oil-droplets to be in contact with the particle surface, as previously reported by several other authors (Linke et al., 2020a; Abd Ghani, Adachi, Sato, et al., 2017). Haas et al. (2019) likewise reported increased free fat for smaller particles in spray-dried powders containing carotenoids. Gharsallaoui et al. (2012) also used pea protein isolate in low concentration (approx. 1.5%) and maltodextrins in the range between DE 6 and DE 28 and obtained free fat values of 15–62.5%, which show the same trend as the presented result.

Free fat was further significantly impacted by maltodextrin Mw and increased with increasing Mw (decreasing DE), a phenomena which has been previously observed in other studies (Sheu & Rosenberg, 1995; Hogan et al., 2001; Danviriyakul et al., 2002). As discussed above (Section 3.1), maltodextrin DE and protein content both impact emulsion viscosity which consecutively influences drying behavior, such as droplet break-up during atomization. Sheu and Rosenberg (1995) and Danviriyakul et al. (2002) both explain changes in free fat content by an increase in oil droplet size from decreasing maltodextrin DE in the feed emulsion, as well as improved stabilization by higher DE-values during spray-drying. For powders with maltodextrin DE 6, surface lipids are visible as large patches on the particle surface while they are being merely located in the fine wrinkles on the particle surface when increasing DE to 40, which could indeed be related to a better stabilization of oil droplets during drying by low molecular weight carbohydrates, providing a more flexible and stress resistant barrier that reduces structural damage of the oil droplets (Danviriyakul et al., 2002) (Fig. 4).

Maltodextrin DE, however, further impacts viscosity of the emulsion system and drives formation of a glassy crust during the spray drying process, which leads to different particle morphologies (Ding et al., 2020; Imamura et al., 2013). Materials with lower viscosity such as high DE maltodextrins have lower diffusivity and thus remain in the rubbery state much longer and can form a continuous network around the oil droplets, whereas long chain polysaccarides such as low DE maltodextrins transition into a glass much more rapidly, hindering the formation of a continuous network and possibly creating more porous structures and surface cracks (Sheu & Rosenberg, 1995; Werner et al., 2007). Hogan et al. (2001) also observed a reduction of free fat for microcapsules with increasing DE maltodextrin as wall material. They

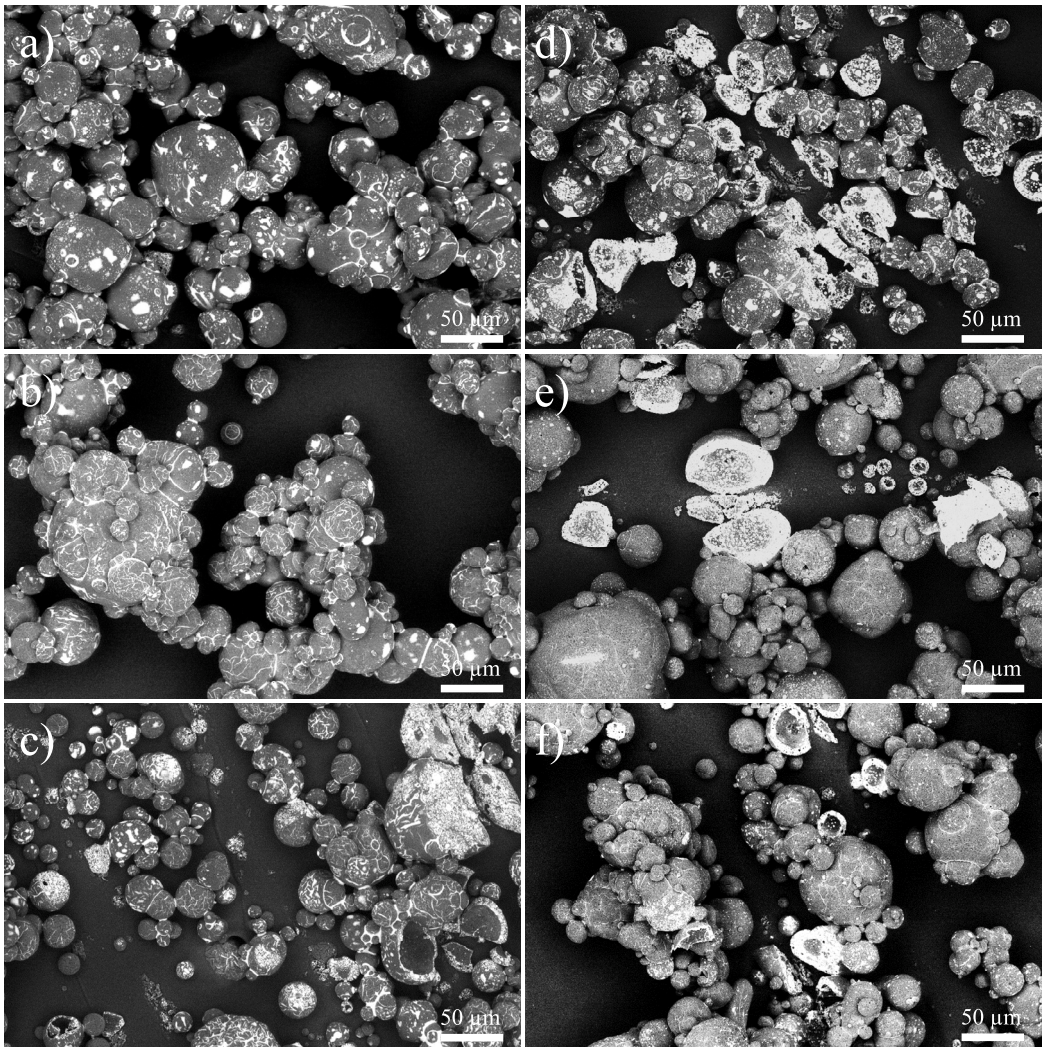

Fig. 4. SEM micrographs of coarse fractions of spray-dried particles with low (a-c) and high (d-f) protein content produced with maltodextrin DE6 (a,b), DE21 (b,e) and DE40 (c,f).

likewise suspected that smaller oligosaccharides in high DE maltodextrins form a less porous, more uniform matrix during drying, which is inaccessible to solvents. Viscosity, as well as glass transition, can also impact the microstructure of spray-dried particles. While there are no observable cracks on the particle surface of the powders produced in this study (Fig. 7), particles do exhibit different morphological characteristics. Particles containing DE 40 maltodextrin are mostly spherical, while DE 6 powders are more irregularly shaped with surface dents. Increased sphericity of powder particles also leads to surface reduction and thus lowers the chance of oil droplets to be in contact with the particle surface which results in a reduction of free fat.

Abd Ghani, Adachi, Shiga, et al. (2017) additionally observed that decreasing DE-value from 25 to 11 promotes the formation of large vacuoles during spray-drying of emulsions and linked these to an increased free fat content. Fig. 7 (c) and (d) similarly show larger vacuoles for DE 6 powder than DE 40 powder. Kikushi et al. (2013) on the other hand simulated the surface oil content of solid and hollow microcapsules and found only a minor influence from a central void. The assumption that free fat content increases with the formation of a cavity inside a spray-dried particle can only be valid if the lipid located inside the vacuole is considered to be extractable. As discussed in Section 2.3, no significant differences in closed porosity between the samples were detected, which would be expected if the vacuoles were fully enclosed within the particle and vacuole size varied with maltodextrin DE. It is thus more likely that the vacuole can be accessed by the solvent through micro channels, increasing the amount of extractable fat.

The increase in free fat from coarse to fine fractions was not proportional across all DE-values. With increasing DE-Value, the increase of free fat from coarse to fine fraction ranged from 27%–45% in DE 6 samples while from 176%–255% in DE 40 samples, which cannot be justified by increasing surface area only. The lower increase for lower DE samples might be related to either a higher share of broken particles with accessible vacuoles or generally a matrix that enables solvent penetration and thus reduces the effect of size.

Concerning protein content, high protein powders generally showed higher free fat content than low protein powders. Although several other studies have investigated the influence of different protein–carbohydrate ratios on encapsulation and free fat (Sheu & Rosenberg, 1998; Hogan et al., 2001; Hogan et al., 2003; Hu et al., 2024), there is no clear answer yet as to how proteins, especially plant proteins, impact free fat content of spray-dried microcapsules. One important aspect to be kept in mind is that increasing pea protein content in formulations also comes with an increase in total lipids from residuals remaining in the protein isolate, which can consequently impact free fat. However, to explain the large differences in free fat content observed in this study, the impact of these lipids does not suffice. Table 4 summarizes the measured $d_{3,2}$ and $d_{4,3}$ mean values of reconstituted emulsions after spray-drying. While values of low protein samples are similar to

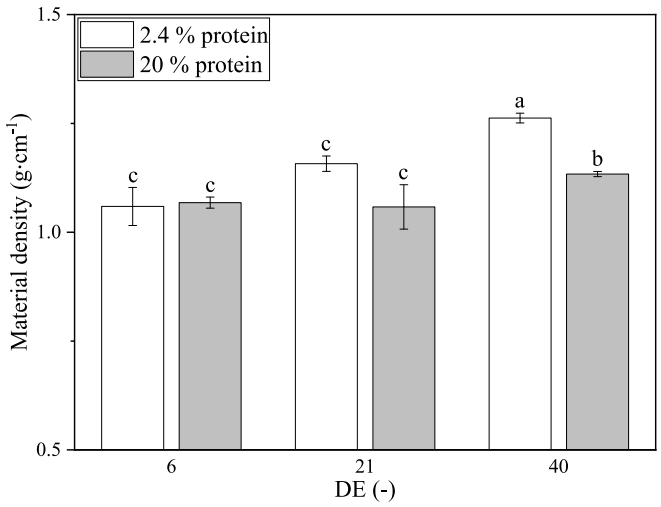

Fig. 5. Material density of formulations with low and high protein content and different maltodextrin DE. Different letters represent significant differences at 0.05 level as determined by one-way ANOVA.

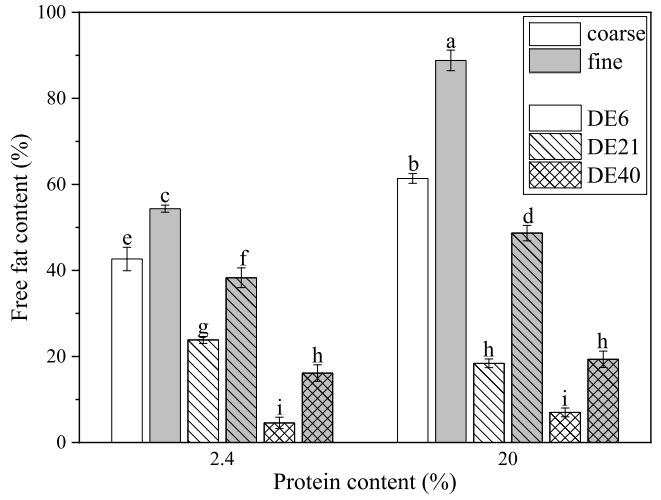

Fig. 6. Free fat content of spray-dried powders after production based on total fat content. Different letters represent significant differences at 0.05 level as determined by one-way ANOVA.

those of the initial emulsion before drying, with only increased $d_{4,3}$ values, those of high protein samples have significantly increased across all samples. It is most likely that the size increase is reflecting the cluster formation of flocculated oil droplets or protein aggregates in the reconstituted emulsion. In Fig. 8, CLSM images of reconstituted emulsions with high and low protein content are shown. In the high protein sample, large green areas as well as red droplet accumulations are visible, indicating the presence of protein aggregates and flocculated droplets. The large protein aggregates form part of the particle wall, disrupting the homogeneous glassy layer of maltodextrin and transforming it into a highly heterogeneous system. This heterogeneous structure could possibly favor the breakage of the emulsion droplets inside the particle and favor their displacement to the particle surface, resulting in higher free fat content. Additionally, Linke et al. (2020c) have shown in a previous study that droplet clusters in the emulsion result in higher non-encapsulated lipids, which can be ascribed to their higher likelihood to be in contact with the particle surface as compared to small emulsion droplets. Hogan et al. (2001) reported

Table 4
Droplet size of reconstituted emulsions before storage.

Protein content (%)	DE (–)	fraction (–)	$d_{3,2}$ (μm)	$d_{4,3}$ (μm)
2.4	6	coarse	8.3 ± 0.3	23.0 ± 0.8
2.4	6	fine	6.7 ± 0.5	16.8 ± 6.6
2.4	21	coarse	7.2 ± 0.8	20.2 ± 4.7
2.4	21	fine	5.6 ± 0.5	9.6 ± 0.6
2.4	40	coarse	7.4 ± 0.5	31.2 ± 16.4
2.4	40	fine	5.3 ± 0.6	11.8 ± 3
20	6	coarse	17.1 ± 2.5	38.5 ± 6.8
20	6	fine	12.0 ± 0.6	20.6 ± 1.2
20	21	coarse	17.4 ± 1.8	40.6 ± 5.7
20	21	fine	12.6 ± 1.0	21.5 ± 2.8
20	40	coarse	14.7 ± 3.6	32.4 ± 5.3
20	40	fine	11.4 ± 1.4	22.2 ± 4.3

higher encapsulation of lipids for microcapsules with higher sodium caseinate content compared to lower ones. They claimed that bulk protein plays a relevant role as solvent barrier in the wall matrix due their hydrophilic nature and therefore prevent the extraction of the hydrophobic lipid core. While this may be true for animal based proteins such as whey protein and sodium caseinate, plant proteins greatly differ in their properties and are generally considered to be hydrophobic (Fernandes et al., 2024). Consequently, the increase of pea protein in the matrix could potentially increase its hydrophobicity and facilitate solvent extraction. This could be particularly relevant since the investigated high-protein samples exhibit large protein-droplet clusters (Fig. 8) as well as non dispersed protein aggregates that may form highly hydrophobic regions from which lipids could be extracted easily even if they were physically "encapsulated" in such a matrix.

3.4. Oxidation stability

Beta carotene content of spray-dried powders was analyzed before and after storage of 84 days under accelerated shelf-life conditions of 35 °C and 20% relative humidity. Due to BC high susceptibility to oxygen, it was used to monitor oxidation stability. In Fig. 9, the retention of total BC (free + encapsulated) in all powders after spray-drying and after storage is displayed. More than 20% of the added BC was degraded during the production process. While low protein powders show no significant difference in BC retention after production, fine fractions of high protein powders exhibit up to 18% higher BC retention than coarse fractions. This difference can be explained through the manufacturing process, during which the cohesive powder particles stuck to the walls of the conical outlet of the drying chamber and had to be extracted through extensive mechanical tapping on the spray dryer walls. The coarse particle fraction had therefore an increased residence time in the spray dryer and longer exposure to the extreme temperatures, which accelerated the degradation of BC, while fine particles were more gently separated through the cyclone. Since free fat as well as protein content can increase powder cohesiveness (Fitzpatrick et al., 2007; Babu et al., 2018), this effect was more pronounced in high protein samples.

There was a slight trend of increased retention with increasing maltodextrin DE, which might be explained by a faster and more efficient encapsulation and film formation (Ding et al., 2020).

For all samples, total BC retention after storage increased with increasing DE value and coarse fractions exhibited a higher retention than fine fractions when related to value after production. In the past, storage stability of encapsulated powders was mostly related to the amount of free fat, since this is known to degrade much more rapidly (e.g. Shiga et al., 2017), however several other studies have shown that non-encapsulated lipids are not always the main driver of lipid oxdiation or degradation of liposoluble components like BC (Drusch & Berg, 2008; Linke et al., 2021). Drusch and Berg (2008) hypothesis that free fat can have a protective effect on encapsulated fat

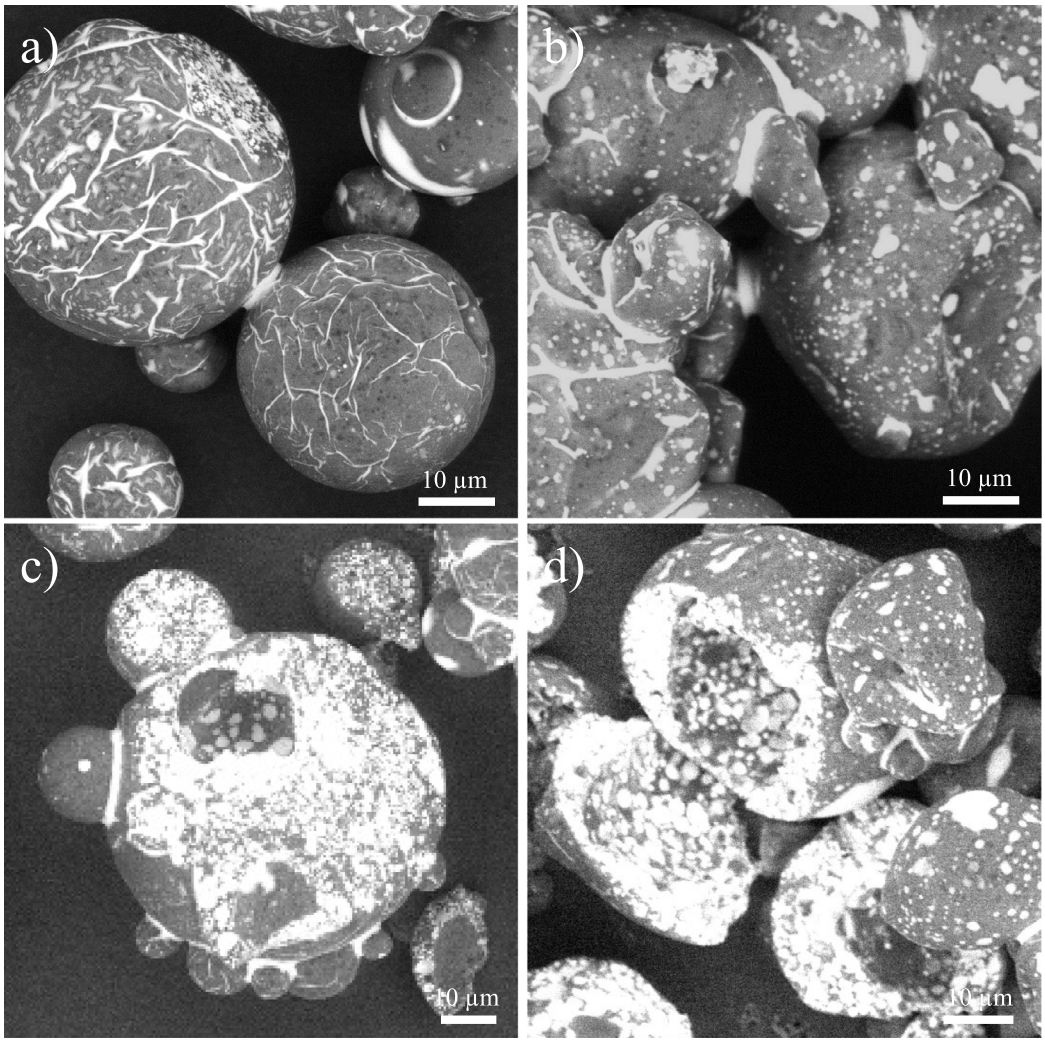

Fig. 7. Close-up SEM micrographs of powder with low protein content and DE40 as exemplary powder with low free fat content (a, c) and high protein content and DE6 exemplary for a powder with high free fat (b,d).

by posing a barrier, whereas Linke et al. (2020d) showed that oxidation of encapsulated lipids contributes to a high extend to the overall lipid oxidation. These findings are in accordance with the data in this study, since free fat contents varied markedly between high and low protein powders, while differences in total BC retention are much smaller. It can be confirmed that encapsulation efficiency was not the sole driver of BC stability of the produced powders, thus it becomes necessary to investigate degradation of free and encapsulated BC separately.

Free BC is the amount of BC that is extractable by heptane from the powder surface and open pores and values generally correlate with the amount of free fat. Free BC is displayed in Fig. 10 as proportion of total BC. Trends for free BC are generally the same as for free fat, with decreasing values for higher maltodextrin DE and larger particle sizes. Degradation of initial free BC was slightly higher in low protein than high protein samples which may be related to possible antioxidant properties of pea protein isolate or a reduced lipid layer thickness due to lower free fat content. Since free BC is not protected from environmental oxygen, it is known to degrade significantly faster than encapsulated BC (Linke et al., 2020d). This can be confirmed, since almost the entire free BC is degraded by the end of storage. Even though free BC is mostly located on the particle surface and is not directly surrounded by protein, it appears that protein can still protect free BC to a certain extend and slightly slow down degradation.

Encapsulated BC represents the amount of BC that is fully embedded within the particle matrix and not directly accessible by solvents or oxygen. The retention of encapsulated BC after 84 days of storage is shown in Fig. 11. For low protein samples, it is possible to identify a positive correlation between maltodextrin DE as well as particle size and encapsulated BC retention, similar to the trend observed for total BC. The positive effect of increased maltodextrin DE on the stability of encapsulated materials such as carotenoids or lipids has been previously reported by other authors (Hogan et al., 2003; Abd Ghani, Adachi, Shiga, et al., 2017). Andersen (2000) encapsulated oil in different carbohydrate matrices by freeze-drying and stated that oxygen permeation through the glassy wall material is crucial for the stability of encapsulated components. Drusch et al. (2009) further measured the free volume elements of different maltodextrins and carbohydrate blends used for encapsulation and determined that there is an exponential correlation between the radius of free volume elements and diffusivity of glassy matrices. As already discussed in Section 2.3, free volume elements and diffusivity therefore decrease with increasing maltodextrin DE, as the reduced carbohydrate chain length enables a denser molecular packing. This is in accordance with the presented results for low protein powders (Fig. 5) and thus explains their increased stability towards oxidation of BC with increasing DE value. For this study, it can be excluded that differences in oxidation result from an increase in air inclusion during drying through viscosity variations from different maltodextrin DE, as proposed by Serfert et al. (2009), since this is not supported by porosity data.

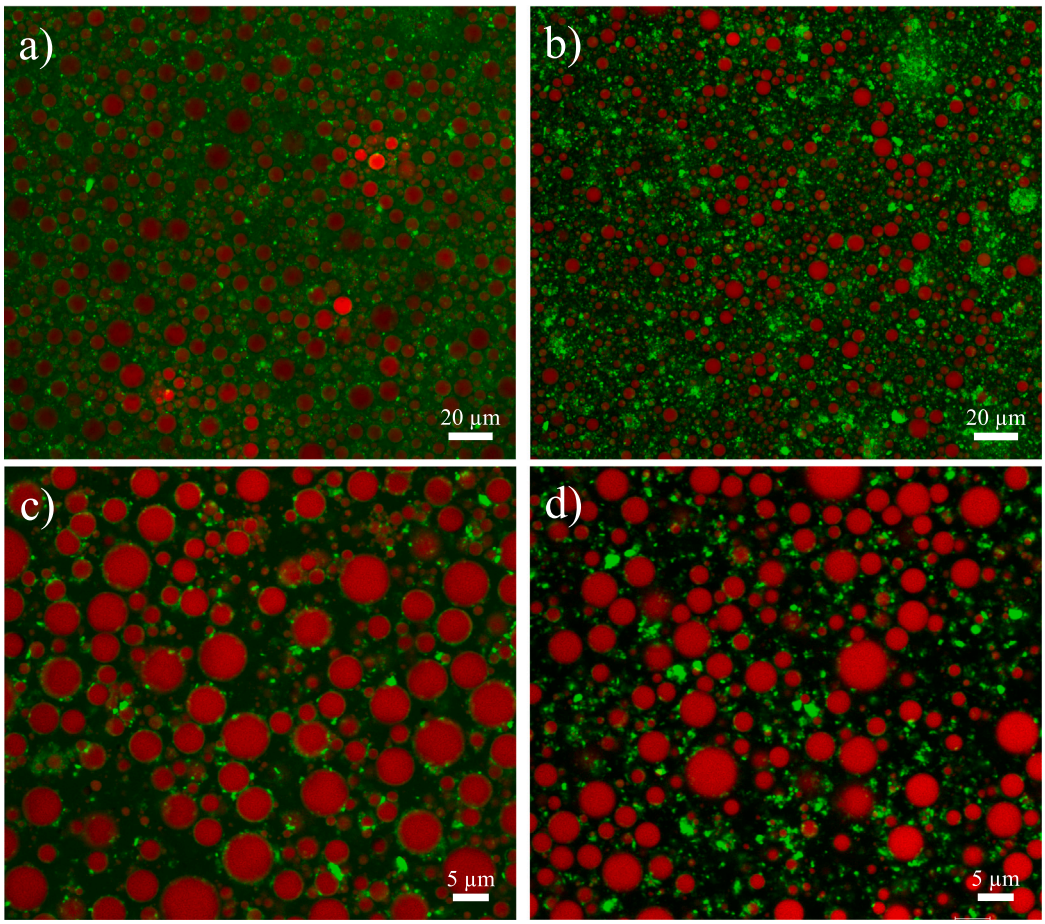

Fig. 8. Confocal laser scanning microscopy images of high and reconstituted powders with low (a, c) and high (b, d) protein powders at different magnifications visualizing proteins (green) and lipids (red).

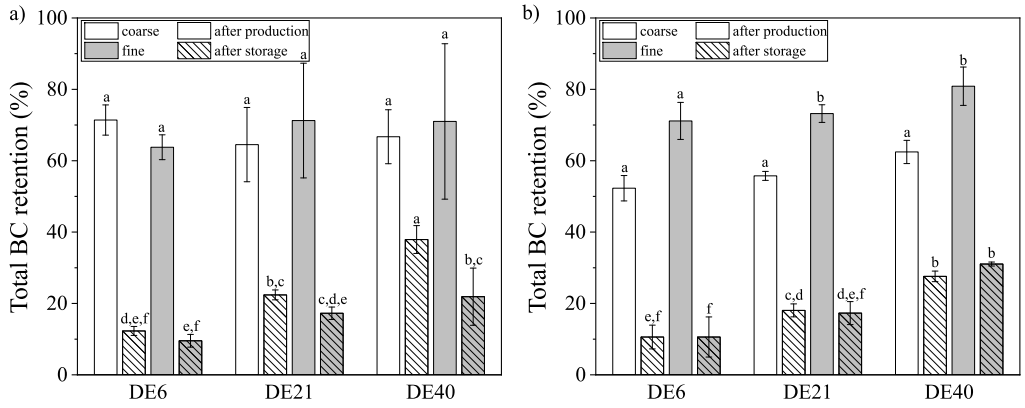

Fig. 9. Retention of total BC after powder production and after storage for 84 days of (a) powders containing 2.4% protein and (b) powders containing 20% protein based on calculated starting concentration in the emulsion. ANOVA was performed individually for samples before and after storage. Different letters represent significant differences at 0.05 level.

Regarding particle size, stability is generally considered to improve with increasing particle size (Haas et al., 2019; Linke et al., 2020b). Haas et al. (2019) established the surface to volume ratio as a crucial impact factor for the stability of carotenoids during storage, whereas Linke et al. (2020b) specified that the effects of interfacial area and penetration both play a critical role for oxidation of encapsulated lipids. Regarding the combination of particle size and maltodextrin DE, it needs to be pointed out that differences in BC retention between coarse and fine fractions increase with increasing maltodextrin DE for low protein samples. This data indicates that matrix diffusivity is the main driving force to prevent oxidation of encapsulated compounds and that particle size mainly becomes relevant when a critical matrix diffusivity is exceeded.

Differences of the BC stability in high protein samples were less pronounced. While there are differences in BC retention between DE 21 and DE 40 samples, no significant differences between the different particle size fractions can be observed. Additionally, the standard deviation for DE 6 powders is extremely high (approx. 20%) and likely caused by the very high free BC, which increases the error in the calculation of encapsulated BC and which further complicates result interpretation.

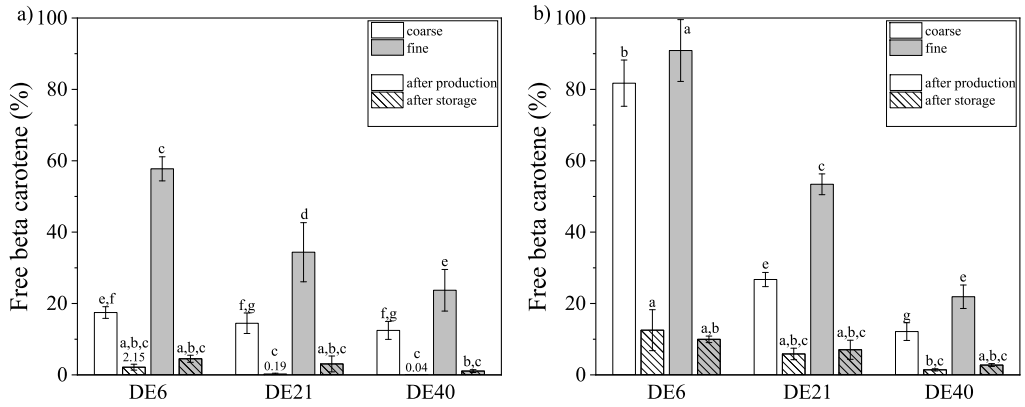

Fig. 10. Fee BC in spray-dried powders after production and after 84 days of storage of (a) powders containing 2.4% protein and (b) powders containing 20% protein. Values represent the ratio to total BC. ANOVA was performed individually for samples before and after storage. Different letters represent significant differences at 0.05 level.

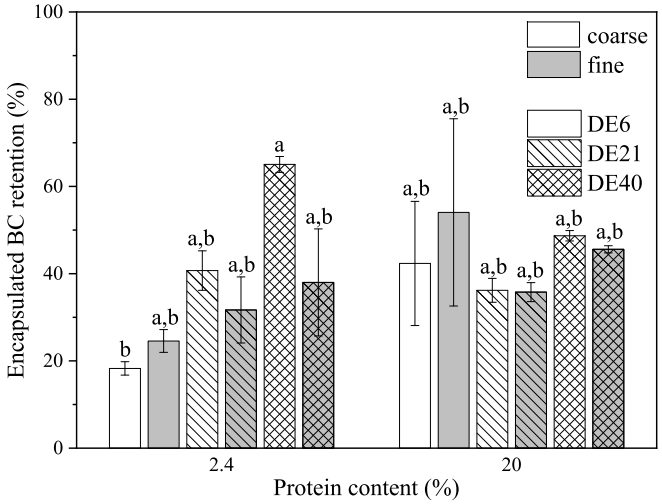

Fig. 11. Retention of encapsulated BC in spray-dried powders after 84 days of storage based on concentration at start of storage. Different letters represent significant differences at 0.05 level.

In another study by Drusch et al. (2012), free volume elements of matrices composed of sodium caseinate and glucose syrup in different ratios were investigated. The authors found that excess protein that is not adsorbed at the oil-matrix interface but rather constitutes part of the matrix, can lead to an increase in free volume elements and might therefore negatively affect oxygen diffusion and stability of encapsulated materials. These findings are generally supported by our observations, as true density of high protein samples is mostly below the one of low protein samples, while differences between the different DE values are reduced. In addition, particle size is not an influencing factor anymore, possibly because matrix density was below the above mentioned critical limit. Following this hypothesis however, it would be expected that encapsulated BC retention would be generally lower in high protein systems, which is not supported by the presented data. Since food systems are highly complex, it has to be assumed that the stability of encapsulated materials is governed by more than one mechanism. One possible explanation is that pea protein has antioxidant capacities and therefore the ability to chemically protect encapsulated BC. Linke et al. (2020a) observed an inverse correlation of droplet size and oxidation products and attributed this to the improved chemical stabilization of soy protein isolate. According to the authors, this stabilization is even more relevant than wall material diffusivity. Carneiro et al. (2013) likewise noted an increased oxidation stability of microcapsules containing whey protein isolate and attributed this to their antioxidant activity. In powdered form, the most relevant antioxidant mechanisms of pea protein are the scavenging of free radicals and quenching of singlet oxygen by endogenous polyphenols or specific amino acids, such as tryptophan, phenylalanine and tyrosine (Wang et al., 2017; D'Alessio et al., 2023; Kim et al., 2025). Another possible explanation could be that, as previously mentioned, the high quantities of free BC may act as an oxygen scavenger and prevent oxygen from penetrating the inside of the particle (Drusch & Berg, 2008). This could also explain the increased retention of high protein DE 6 samples. While high quantities of free fat can enhance the protection of encapsulated lipids, it is however not a recommended process route, since non-volatile compounds formed during oxidation of non-encapsulated lipids can be easily released from the powder surface, leading to undesired organoleptic properties.

4. Conclusion

This study investigates the critical influence of both pea protein content and maltodextrin molecular weight on the structure and stability of spray-dried emulsions. Despite achieving consistent oil droplet sizes across different formulations prior to drying, high protein samples exhibited increased levels of undissolved protein aggregates—particularly as maltodextrin molecular weight increased (decreasing DE). These aggregates significantly impacted the free fat content, spanning a broad range from 4.5 to 88.8%, due to the susceptibility for droplet clustering and protein aggregation, which increased fat extractability.

The stability analysis over an 84-day period showed that dried emulsions with low protein content and high DE maltodextrin retained the highest levels of total beta carotene at 37.9%. Encapsulated beta carotene retention improved as maltodextrin molecular weight decreased, underscoring the importance of wall material diffusivity. However, high protein formulations demonstrated minimal sensitivity to maltodextrin DE and no observable influence of particle size on beta carotene retention, suggesting that plant proteins and aggregates might enhance wall diffusivity, facilitating oxidative degradation. Notably, increased pea protein isolate might enhance oxidative stability due to potential antioxidant properties.

This research highlights the challenges in formulating stable milk alternatives with high plant protein content. To ensure a prolonged shelf life while maintaining adequate protein levels, further stabilization of the emulsion system is necessary, potentially through additional emulsifiers. Additionally, next to oxidation stability, rehydration and powder dispersibility are crucial for shelf-life optimization and should be prioritized in future research and formulation.

CRediT authorship contribution statement

T. Kurtz: Writing – original draft, Visualization, Validation, Methodology, Investigation, Formal analysis, Data curation, Conceptualization. **K. Haas:** Writing – review & editing, Supervision, Project administration, Methodology, Conceptualization. **J. Busom Descarrega:** Writing – review & editing, Methodology, Investigation. **V. Meunier:** Writing – review & editing, Supervision, Project administration. **O. Schafer:** Supervision, Project administration, Methodology. **S. Heinrich:** Writing – review & editing, Supervision, Project administration, Funding acquisition.

Declaration of competing interest

The authors declare that they have no known competing financial interests or personal relationships that could have appeared to influence the work reported in this paper.

Acknowledgments

This work was supported by Nestlé Research. The authors would like to thank Carine Morgenegg for the confocal microscopy analysis. The authors would like to further thank Elmira Rastifard and Alina Raza for their support with data acquisition.

Appendix A. Supplementary data

Supplementary material related to this article can be found online at https://doi.org/10.1016/j.foodhyd.2025.111320.

Data availability

Data will be made available on request.

References

Abd Ghani, A., Adachi, S., Sato, K., Shiga, H., Iwamoto, S., Neoh, T. L., Adachi, S., & Yoshii, H. (2017). Effects of oil-droplet diameter and dextrose equivalent of maltodextrin on the surface-oil ratio of microencapsulated fish oil by spray drying. *Journal of Chemical Engineering of Japan*, *50*(10), 799–806. http://dx.doi.org/10.1252/jcej.17we048.

Abd Ghani, A., Adachi, S., Shiga, H., Neoh, T. L., Adachi, S., & Yoshii, H. (2017). Effect of different dextrose equivalents of maltodextrin on oxidation stability in encapsulated fish oil by spray drying. *Bioscience, Biotechnology, and Biochemistry*, *81*(4), 705–711. http://dx.doi.org/10.1080/09168451.2017.1281721.

Akharume, F. U., Aluko, R. E., & Adedeji, A. A. (2021). Modification of plant proteins for improved functionality: A review. *Comprehensive Reviews in Food Science and Food Safety*, *20*(1), 198–224. http://dx.doi.org/10.1111/1541-4337.12688.

An, N., Li, X., Ji, G., Liu, J., Zhu, X., Li, N., Wang, Z., Mu, Z., & Liu, H. (2024). A comprehensive review on composition to application of pea protein and its components. *International Journal of Biological Macromolecules*, *282*(Pt 5), Article 137273. http://dx.doi.org/10.1016/j.ijbiomac.2024.137273.

Andersen, A. (2000). Oxygen permeation through an oil-encapsulating glassy food matrix studied by ESR line broadening using a nitroxyl spin probe. *Food Chemistry*, *70*(4), 499–508. http://dx.doi.org/10.1016/S0308-8146(00)00102-3.

Avaltroni, F., Bouquerand, P., & Normand, V. (2004). Maltodextrin molecular weight distribution influence on the glass transition temperature and viscosity in aqueous solutions. *Carbohydrate Polymers*, *58*(3), 323–334. http://dx.doi.org/10.1016/j.carbpol.2004.08.001.

Aydar, E. F., Tutuncu, S., & Ozcelik, B. (2020). Plant-based milk substitutes: Bioactive compounds, conventional and novel processes, bioavailability studies, and health effects. *Journal of Functional Foods*, *70*, Article 103975. http://dx.doi.org/10.1016/j.jff.2020.103975.

Babu, K. S., Siliveru, K., Amamcharla, J. K., Vadlani, P. V., & Ambrose, R. P. K. (2018). Influence of protein content and storage temperature on the particle morphology and flowability characteristics of milk protein concentrate powders. *Journal of Dairy Science*, *101*(8), 7013–7026. http://dx.doi.org/10.3168/jds.2018-14405.

Bernaschina, M., Leser, M. E., Limbach, H. J., Fischer, P., & Roucher, A. (2024). Lentil protein stabilized emulsion - impact of lecithin addition on emulsions properties. *Food Hydrocolloids*, *147*, Article 109337. http://dx.doi.org/10.1016/j.foodhyd.2023.109337.

Binesh, N., Babaloo, H., & Farhadian, N. (2023). Microencapsulation: Spray drying. In F. Sefat, G. Farzi, & M. Mozafar (Eds.), *Principles of biomaterials encapsulation* (pp. 271–296). Cambridge, MA, United States: Woodhead Publishing.

Boukid, F., Rosell, C. M., Rosene, S., Bover-Cid, S., & Castellari, M. (2022). Non-animal proteins as cutting-edge ingredients to reformulate animal-free foodstuffs: Present status and future perspectives. *Critical Reviews in Food Science and Nutrition*, *62*(23), 6390–6420. http://dx.doi.org/10.1080/10408398.2021.1901649.

Brunauer, S., Emmett, P. H., & Teller, E. (2000). Adsorption of gases in multimolecular layers. *Polymers for Advanced Technology*, *11*, 766–771.

Buma, T. J. (1971). Free fat and physical structure of spray-dried whole milk: 10. a final report with a physical model for free fat in spray-dried milk. *Netherlands Milk and Dairy Journal*, *25*, 53–72.

Burger, T. G., Singh, I., Mayfield, C., Baumert, J. L., & Zhang, Y. (2022). Comparison of physicochemical and emulsifying properties of commercial pea protein powders. *Journal of the Science of Food and Agriculture*, *102*(6), 2506–2514. http://dx.doi.org/10.1002/jsfa.11592.

Burger, T. G., & Zhang, Y. (2019). Recent progress in the utilization of pea protein as an emulsifier for food applications. *Trends in Food Science & Technology*, *86*, 25–33. http://dx.doi.org/10.1016/j.tifs.2019.02.007.

Cao, X., Wang, S., Yu, Y., Han, L., & Liu, H. (2025). Enhancing emulsification properties of pea protein isolate: Impact of heat treatment and soy hull polysaccharides on conformational modification and stability. *International Journal of Biological Macromolecules*, Article 140106. http://dx.doi.org/10.1016/j.ijbiomac.2025.140106.

Carneiro, H. C., Tonon, R. V., Grosso, C. R., & Hubinger, M. D. (2013). Encapsulation efficiency and oxidative stability of flaxseed oil microencapsulated by spray drying using different combinations of wall materials. *Journal of Food Engineering*, *115*(4), 443–451. http://dx.doi.org/10.1016/j.jfoodeng.2012.03.033.

Coccaro, N., Ferrari, G., & Donsì, F. (2018). Understanding the break-up phenomena in an orifice-valve high pressure homogenizer using spherical bacterial cells (lactococcus lactis) as a model disruption indicator. *Journal of Food Engineering*, *236*, 60–71. http://dx.doi.org/10.1016/j.jfoodeng.2018.05.011.

D'Alessio, G., Flamminii, F., Faieta, M., Prete, R., Di Michele, A., Pittia, P., & Di Mattia, C. D. (2023). High pressure homogenization to boost the technological functionality of native pea proteins. *Current Research in Food Science*, *6*, Article 100499. http://dx.doi.org/10.1016/j.crfs.2023.100499.

Danviriyakul, S., McClements, D., Decker, E., Nawar, W., & Chinachoti, P. (2002). Physical stability of spray-dried milk fat emulsion as affected by emulsifiers and processing conditions. *Journal of Food Science*, *67*(6), 2183–2189.

de Barros Fernandes, R. V., Marques, G. R., Borges, S. V., & Botrel, D. A. (2014). Effect of solids content and oil load on the microencapsulation process of rosemary essential oil. *Industrial Crops and Products*, *58*, 173–181. http://dx.doi.org/10.1016/j.indcrop.2014.04.025.

Ding, Z., Tao, T., Wang, X., Prakash, S., Zhao, Y., Han, J., & Wang, Z. (2020). Influences of different carbohydrates as wall material on powder characteristics, encapsulation efficiency, stability and degradation kinetics of microencapsulated lutein by spray drying. *International Journal of Food Science & Technology*, *55*(7), 2872–2882. http://dx.doi.org/10.1111/ijfs.14544.

Dlubek, G., Stejny, J., Lüpke, T., Bamford, D., Petters, K., Hübner, C., Alam, M. A., & Hill, M. J. (2002). Free–volume variation in polyethylenes of different crystallinities: Positron lifetime, density, and X–ray studies. *Journal of Polymer Science Part B: Polymer Physics*, *40*(1), 65–81. http://dx.doi.org/10.1002/polb.10072.

Drusch, S., & Berg, S. (2008). Extractable oil in microcapsules prepared by spray-drying: Localisation, determination and impact on oxidative stability. *Food Chemistry*, *109*(1), 17–24. http://dx.doi.org/10.1016/j.foodchem.2007.12.016.

Drusch, S., Rätzke, K., Shaikh, M. Q., Serfert, Y., Steckel, H., Scampicchio, M., Voigt, I., Schwarz, K., & Mannino, S. (2009). Differences in free volume elements of the carrier matrix affect the stability of microencapsulated lipophilic food ingredients. *Food Biophysics*, *4*(1), 42–48. http://dx.doi.org/10.1007/s11483-008-9100-9.

Drusch, S., Serfert, Y., Berger, A., Shaikh, M. Q., Rätzke, K., Zaporojtchenko, V., & Schwarz, K. (2012). New insights into the microencapsulation properties of sodium caseinate and hydrolyzed casein. *Food Hydrocolloids*, *27*(2), 332–338. http://dx.doi.org/10.1016/j.foodhyd.2011.10.001.

Dupas-Langlet, M., Dupas, J., Samain, S., Giardiello, M.-I., Meunier, V., & Forny, L. (2016). A new method to determine "equilibrated" water activity and establish sorption isotherm by erasing surface history of the samples. *Journal of Food Engineering*, *184*, 53–62. http://dx.doi.org/10.1016/j.jfoodeng.2016.03.023.

Fang, X., Shima, M., & Adachi, S. (2005). Effects of drying conditions on the oxidation of linoleic acid encapsulated with gum arabic by spray-drying. *Food Science and Technology Research*, *11*(4), 380–384. http://dx.doi.org/10.3136/fstr.11.380.

Fernandes, J. G., Rodrigues, R. C., Pereira, L., Stringheta, P. C., Campelo, P. H., & Martins, E. (2024). Encapsulation of hydrophobic active ingredients in plant proteins: modulation of interfacial properties and encapsulation efficiency. *Current Opinion in Food Science*, *57*, Article 101170. http://dx.doi.org/10.1016/j.cofs.2024.101170.

Fitzpatrick, J. J., Barry, K., Cerqueira, P., Iqbal, T., O'Neill, J., & Roos, Y. H. (2007). Effect of composition and storage conditions on the flowability of dairy powders. *International Dairy Journal*, *17*(4), 383–392. http://dx.doi.org/10.1016/j.idairyj.2006.04.010.

Gavi, E., Kubicki, D., Padron, G. A., & Özcan-Taşkın, N. G. (2018). Breakup of nanoparticle clusters using microfluidizer M110-p. *Chemical Engineering Research and Design*, *132*, 902–912. http://dx.doi.org/10.1016/j.cherd.2018.01.011.

Gharsallaoui, A., Saurel, R., Chambin, O., & Voilley, A. (2012). Pea (pisum sativum, l.) protein isolate stabilized emulsions: A novel system for microencapsulation of lipophilic ingredients by spray drying. *Food and Bioprocess Technology*, *5*(6), 2211–2221. http://dx.doi.org/10.1007/s11947-010-0497-z.

Gianfrancesco, A., Vuataz, G., Mesnier, X., & Meunier, V. (2012). New methods to assess water diffusion in amorphous matrices during storage and drying. *Food Chemistry*, *132*(4), 1664–1670. http://dx.doi.org/10.1016/j.foodchem.2011.06.058.

Gordon, M., & Taylor, J. S. (1952). Ideal copolymers and the second–order transitions of synthetic rubbers. i. non–crystalline copolymers. *Journal of Applied Chemistry*, *2*(9), 493–500. http://dx.doi.org/10.1002/jctb.5010020901.

Haas, K., Dohnal, T., Andreu, P., Zehetner, E., Kiesslich, A., Volkert, M., Fryer, P., & Jaeger, H. (2020). Particle engineering for improved stability and handling properties of carrot concentrate powders using fluidized bed granulation and agglomeration. *Powder Technology*, *370*, 104–115. http://dx.doi.org/10.1016/j.powtec.2020.04.065.

Haas, K., Obernberger, J., Zehetner, E., Kiesslich, A., Volkert, M., & Jaeger, H. (2019). Impact of powder particle structure on the oxidation stability and color of encapsulated crystalline and emulsified carotenoids in carrot concentrate powders. *Journal of Food Engineering*, *263*, 398–408. http://dx.doi.org/10.1016/j.jfoodeng.2019.07.025.

Hinderink, E. B. A., Berton-Carabin, C. C., Schroën, K., Riaublanc, A., Houinsou-Houssou, B., Boire, A., & Genot, C. (2021). Conformational changes of whey and pea proteins upon emulsification approached by front-surface fluorescence. *Journal of Agricultural and Food Chemistry*, *69*(23), 6601–6612. http://dx.doi.org/10.1021/acs.jafc.1c01005.

Hinderink, E. B., Schröder, A., Sagis, L., Schroën, K., & Berton-Carabin, C. C. (2021). Physical and oxidative stability of food emulsions prepared with pea protein fractions. *LWT*, *146*, Article 111424. http://dx.doi.org/10.1016/j.lwt.2021.111424.

Hogan, S. A., McNamee, B. F., O'Riordan, E. D., & O'Sullivan, M. (2001). Emulsification and microencapsulation properties of sodium caseinate/carbohydrate blends. *International Dairy Journal*, *11*, 137–144.

Hogan, S. A., O'Riordan, E. D., & O'Sullivan, M. (2003). Microencapsulation and oxidative stability of spray-dried fish oil emulsions. *Journal of Microencapsulation*, *20*(5), 675–688. http://dx.doi.org/10.3109/02652040309178355.

Hu, Y., Tu, J., Li, C., Peng, J., Xiao, Z., Wen, L., Chen, Y., Xie, S., Liu, S., & Xiao, J. (2024). Microencapsulation of camellia seed oil by spray drying with pea protein and maltodextrin. *LWT*, *203*, Article 116348. http://dx.doi.org/10.1016/j.lwt.2024.116348.

Imamura, K., Kimura, Y., Nakayama, S., Sayuri, M., Ogawa, S., Hoshino, T., Oshitani, J., Kobayashi, T., Adachi, S., Matsuura, T., Imanaka, H., Ishida, N., & Nakanishi, K. (2013). Characteristics of amorphous matrices composed of different types of sugars in encapsulating emulsion oil droplets during freeze-drying. *Food Research International*, *51*(1), 201–207. http://dx.doi.org/10.1016/j.foodres.2012.12.010.

Jafari, S. M., He, Y., & Bhandari, B. (2007). Role of powder particle size on the encapsulation efficiency of oils during spray drying. *Drying Technology*, *25*(6), 1081–1089. http://dx.doi.org/10.1080/07373930701397343.

Keuleyan, E., Gélébart, P., Beaumal, V., Kermarrec, A., Ribourg-Birault, L., Le Gall, S., Meynier, A., Riaublanc, A., & Berton-Carabin, C. (2023). Pea and lupin protein ingredients: New insights into endogenous lipids and the key effect of high-pressure homogenization on their aqueous suspensions. *Food Hydrocolloids*, *141*, Article 108671. http://dx.doi.org/10.1016/j.foodhyd.2023.108671.

Kikushi, K., Yamamoto, S., Shiga, H., Yoshii, H., & Adachi, S. (2013). Surface oil content of microcapsules containing various oil fractions and oil-droplet sizes. *Japan Journal of Food Engineering*, *14*(4), 169–173.

Kim, E. H.-J., Chen, X. D., & Pearce, D. (2009). Surface composition of industrial spray-dried milk powders. 2. Effects of spray drying conditions on the surface composition. *Journal of Food Engineering*, *94*(2), 169–181. http://dx.doi.org/10.1016/j.jfoodeng.2008.10.020.

Kim, W., Zia, M. B., Naik, R. R., Ho, K. K. H. Y., & Selomulya, C. (2025). Effects of polyphenols from tasmannia lanceolata on structural, emulsifying, and antioxidant properties of pea protein. *Food Chemistry*, *464*(Pt 1), Article 141589. http://dx.doi.org/10.1016/j.foodchem.2024.141589.

Kramm, K., Roucher, A., Busom Descarrega, J., Ambühl, M., Kammerhofer, J., Meunier, V., & Heinrich, S. (2024). Influence of material characteristics on plant-based milk alternative properties. *Journal of Food Engineering*, *373*, Article 112019. http://dx.doi.org/10.1016/j.jfoodeng.2024.112019.

Laina, K. T., Drosou, C., & Krokida, M. (2024). Comparative assessment of encapsulated essential oils through the innovative electrohydrodynamic processing and the conventional spray drying, and freeze-drying techniques. *Innovative Food Science & Emerging Technologies*, *95*, Article 103720. http://dx.doi.org/10.1016/j.ifset.2024.103720.

Linke, A., Hinrichs, J., & Kohlus, R. (2020a). Impact of the oil droplet size on the oxidative stability of microencapsulated oil. *Journal of Microencapsulation*, *37*(2), 170–181. http://dx.doi.org/10.1080/02652048.2020.1713243.

Linke, A., Hinrichs, J., & Kohlus, R. (2020b). Impact of the powder particle size on the oxidative stability of microencapsulated oil. *Powder Technology*, *364*, 115–122. http://dx.doi.org/10.1016/j.powtec.2020.01.077.

Linke, A., Weiss, J., & Kohlus, R. (2020c). Factors determining the surface oil concentration of encapsulated lipid particles: impact of the emulsion oil droplet size. *European Food Research and Technology*, *246*(10), 1933–1943. http://dx.doi.org/10.1007/s00217-020-03545-5.

Linke, A., Weiss, J., & Kohlus, R. (2020d). Oxidation rate of the non-encapsulated- and encapsulated oil and their contribution to the overall oxidation of microencapsulated fish oil particles. *Food Research International (Ottawa, Ont.)*, *127*, Article 108705. http://dx.doi.org/10.1016/j.foodres.2019.108705.

Linke, A., Weiss, J., & Kohlus, R. (2021). Impact of the oil load on the oxidation of microencapsulated oil powders. *Food Chemistry*, *341*(Pt 1), Article 128153. http://dx.doi.org/10.1016/j.foodchem.2020.128153.

McClements, D. J., Newman, E., & McClements, I. F. (2019). Plant-based milks: A review of the science underpinning their design, fabrication, and performance. *Comprehensive Reviews in Food Science and Food Safety*, *18*(6), 2047–2067. http://dx.doi.org/10.1111/1541-4337.12505.

Palade, G. E. (1951). A study of fixation for electron microscopy. *The Journal of Experimental Medicine*, *95*, 285–298.

Rodríguez-Hernández, G. R., González-García, R., Grajales-Lagunes, A., Ruiz-Cabrera*, M. A., & Abud-Archila, M. (2005). Spray-drying of cactus pear juice (opuntia streptacantha): Effect on the physicochemical properties of powder and reconstituted product. *Drying Technology*, *23*(4), 955–973. http://dx.doi.org/10.1080/DRT-200054251.

Sarkar, A., Arfsten, J., Golay, P.-A., Acquistapace, S., & Heinrich, E. (2016). Microstructure and long-term stability of spray dried emulsions with ultra-high oil content. *Food Hydrocolloids*, *52*, 857–867. http://dx.doi.org/10.1016/j.foodhyd.2015.09.003.

Schröder, J., Kleinhans, A., Serfert, Y., Drusch, S., Schuchmann, H. P., & Gaukel, V. (2012). Viscosity ratio: A key factor for control of oil drop size distribution in effervescent atomization of oil-in-water emulsions. *vol. 111*, http://dx.doi.org/10.1016/j.jfoodeng.2012.02.023.

Schumacher, T., Steinmacher, T., Köster, E., Wagemans, A., Weiss, J., & Gibis, M. (2025). Physico-chemical characterization of ten commercial pea protein isolates. *Food Hydrocolloids*, *162*, Article 110996. http://dx.doi.org/10.1016/j.foodhyd.2024.110996.

Serfert, Y., Drusch, S., Schmidt-Hansberg, B., Kind, M., & Schwarz, K. (2009). Process engineering parameters and type of n-octenylsuccinate-derivatised starch affect oxidative stability of microencapsulated long chain polyunsaturated fatty acids. *Journal of Food Engineering*, *95*(3), 386–392. http://dx.doi.org/10.1016/j.jfoodeng.2009.05.021.

Sethi, S., Tyagi, S. K., & Anurag, R. K. (2016). Plant-based milk alternatives an emerging segment of functional beverages: a review. *Journal of Food Science and Technology*, *53*(9), 3408–3423. http://dx.doi.org/10.1007/s13197-016-2328-3.

Sheu, T.-Y., & Rosenberg, M. (1995). Microencapsulation by spray drying ethyl caprylate in whey protein and carbohydrate wall systems. *Journal of Food Science*, *60*(1), 98–103.

Sheu, T.-Y., & Rosenberg, M. (1998). Microstructure of microcapsules consisting of whey proteins and carbohydrates. *Journal of Food Science*, *63*(3), 491–494.

Shiga, H., Loon Neoh, T., Ninomiya, A., Adachi, S., Pasten, I. L., Adachi, S., & Yoshii, H. (2017). Effect of oil droplet size on the oxidative stability of spray-dried flaxseed oil powders. *Bioscience, Biotechnology, and Biochemistry*, *81*(4), 698–704. http://dx.doi.org/10.1080/09168451.2017.1281720.

Vogelsang-O'Dwyer, M., Sahin, A. W., Arendt, E. K., & Zannini, E. (2022). Enzymatic hydrolysis of pulse proteins as a tool to improve techno-functional properties. *Foods (Basel, Switzerland)*, *11*(9), http://dx.doi.org/10.3390/foods11091307.

Wang, L., Zhang, X., Liu, F., Ding, Y., Wang, R., Luo, X., Li, Y., & Chen, Z. (2017). Study of the functional properties and anti-oxidant activity of pea protein irradiated by electron beam. *Innovative Food Science & Emerging Technologies*, *41*, 124–129. http://dx.doi.org/10.1016/j.ifset.2017.01.005.

Werner, S. R., Jones, J. R., & Paterson, A. H. (2007). Stickiness of maltodextrins using probe tack test during in-situ drying. *Journal of Food Engineering*, *80*(3), 859–868. http://dx.doi.org/10.1016/j.jfoodeng.2006.08.008.

Yang, J., Kornet, R., Ntone, E., Meijers, M. G., van den Hoek, I. A., Sagis, L. M., Venema, P., Meinders, M. B., Berton-Carabin, C. C., Nikiforidis, C. V., & Hinderink, E. B. (2024). Plant protein aggregates induced by extraction and fractionation processes: Impact on techno-functional properties. *Food Hydrocolloids*, *155*, Article 110223. http://dx.doi.org/10.1016/j.foodhyd.2024.110223.